General Disclaimer

One or more of the Following Statements may affect this Document

- This document has been reproduced from the best copy furnished by the organizational source. It is being released in the interest of making available as much information as possible.

- This document may contain data, which exceeds the sheet parameters. It was furnished in this condition by the organizational source and is the best copy available.

- This document may contain tone-on-tone or color graphs, charts and/or pictures, which have been reproduced in black and white.

- This document is paginated as submitted by the original source.

- Portions of this document are not fully legible due to the historical nature of some of the material. However, it is the best reproduction available from the original submission.

NASA TECHNICAL MEMORANDUM

NASA TM X-73533

NASA TM X-73533

SPUTTERING PHENOMENA OF DISCHARGE CHAMBER COMPONENTS IN A 30-CM DIAMETER HG ION THRUSTER

by Maris A. Mantenieks and Vincent K. Rawlin
Lewis Research Center
Cleveland, Ohio 44135

TECHNICAL PAPER to be presented at the
Twelfth International Electric Propulsion Conference sponsored by the
American Institute of Aeronautics and Astronautics
Key Biscayne, Florida, November 15-17, 1976

SPUTTERING PHENOMENA OF DISCHARGE CHAMBER COMPONENTS IN A 30-CM DIAMETER HG ION THRUSTER

Maris A. Mantenieks and Vincent K. Rawlin
National Aeronautics and Space Administration
Lewis Research Center
Cleveland, Ohio 44135

Abstract

Sputtering and deposition rates have been measured for discharge chamber components of a 30-cm diameter mercury ion thruster. It was found that sputtering rates of the screen grid and cathode baffle were strongly affected by geometry of the baffle holder. Sputtering rates of the baffle and screen grid were reduced to 80 and 125 A/hr, respectively, by combination of appropriate geometry and materials selections. Sputtering rates such as these are commensurate with thruster lifetimes of 15 000 hours or more. A semi-empirical sputtering model showed good agreement with the measured values.

Introduction

Electron bombardment thrusters have been proposed for a variety of missions for both station-keeping and attitude control[1,2] as well as primary propulsion.[3,4] In general, these missions require thruster lifetimes, and associated performance and control stability, for periods of 15 000 hours or greater. A number of tests have been carried out to identify the life limiting characteristics of these thrusters. These tests have indicated that sputtering of the discharge chamber components and subsequent spalling of films of sputtered material are two of the most important life limiting phenomena in electron bombardment thrusters.

E-8957

For example, considerable internal erosion and subsequent spalling was observed in a recently completed 10 000 hour life test of a 30 cm diameter thruster.[5] The detrimental effects of internal erosion were also observed in lifetests with the 5 and 8 cm electron bombardment thrusters.[6,7] In particular, this phenomena was responsible for grid damage and subsequent thruster shutdown in a 9 700 hour test of a 5 cm diameter thruster.[6]

Several studies have been performed to characterize and eliminate the adverse effects of internal erosion in both the 8 and 30 cm diameter thrusters.[7,8,9,10] From these studies a large number of thruster design and/or operating modifications have been defined and verified. These modifications consisted basically of (1) the use of lower sputter yield materials at identified erosion sites; (2) special surface treatment of identified deposition sites to improve film adhesion and/or control the size of spalled material; and (3) certain thruster operating condition modifications to reduce the magnitude of sputter erosion. The use of these modifications has been recently verified for the 8-cm thruster by the successful completion of a 15 000 hour lifetest wherein no detrimental effects due to discharge chamber sputter erosion were observed.[11]

The results of preliminary internal erosion studies for the 30 cm thruster[8] indicated that erosion of the baffle and cathode pole piece can be reduced to acceptable levels. However, the completed 10 000 lifetest[5] indicated that the erosion of the screen grid may limit thruster lifetime to periods shorter than those required by the proposed missions.

This paper presents the results of a program performed to characterize and provide solutions to the sputtering-deposition problems in a 30 cm diameter thruster. Erosion rates were evaluated for various critical erosion sites with a variety of component materials and configurations over a range of thruster operating conditions. Deposition rates were measured inside the thruster in order to identify deposition sites as well as assess the impact of deposition on sputtering rates of components that undergo both deposition and sputtering. A semi-empirical model for erosion and deposition of thruster components was made and the results were compared to the test results. This effort was part of the definition of the present 30 cm Engineering Model Thruster (EMT).[12] Estimates of expected lifetimes of the discharge chamber components were made. Although the work presented herein was specific to the 30 cm thruster it is felt that the approach used in defining and reducing the adverse effects of sputtering and deposition phenomena are applicable to other plasma systems which may suffer similar life limiting phenomena.

Apparatus and Procedure

Thrusters

Figure 1 shows a cross section view of a typical 30 cm diameter thruster. Several thrusters, using different components, were used to expedite the study. In these studies it became apparent that the geometries, materials, and electrical operating parameters all played significant roles in the internal sputtering-spalling problems. Components which were found to significantly influence the sputtering rate of internal thruster components were thruster optics, baffle mount, and baffle geometry and material. These components will be described here in detail in order to allow comparisons of sputtering rates with various thrusters.

Table I(a) shows a summary of the sputtering tests, thruster and thruster components used along with the operating conditions and duration of each test. Table I(b) describes each thruster with its designated serial number. The first thruster used was 406 A which was a modified 400 series thruster.[13,14] The modifications were a result of performance studies involving the use of dished ion optics, a stronger magnetic field and a shortened baffle mount.[13] The "700" series thruster evolved from the modified "400" series thruster with changes to the thruster external structure, separation of the cathode from the isolator-vaporizer assembly, and further modification to the baffle mount.[15] Figure 2 shows the dimensional variations between the "400" and "700" geometry baffle mounts. The

STAR category 20

"800" series thrusters were similar to the "700" series except for modifications of the external thruster structure for mechanical integrity improvements.[16] The present 900 series thrusters[12] incorporate modifications of the internal thruster components to minimize sputtering-spalling effects. These include cladding the deposition sites such as the anode and backplate with grit blasted wire mesh, cladding the baffle, baffle mount and cathode pole piece with tantalum and reverting back to the use of the modified 400 series baffle mount.

The geometry of the ion accelerating systems for all of the tests presented herein had screen grid and accelerator grid hole diameter of 0.19 and 0.15 cm, respectively, and grid thicknesses of 0.038 and 0.051 cm, respectively. The open area fraction of the screen grid was 0.67 while that of the accelerator was 0.43. To compensate for beam divergence the screen grid hole pattern was scaled down by 0.4 percent for all optics except set 32 where it was reduced by 0.5 percent.

Table I(c) lists the baffle and pole piece materials and geometries for each test. A single iron baffle was used during the 10 000 hour lifetest. A variety of multilayered baffle configurations were used in tests 2 and 3. Those configurations used in test 3 were reported in reference 8. Tests 4, 5, 11, and 12 utilized the 900 series baffle geometry, shown in figure 3(a), wherein the magnetic mild steel baffle is entirely covered with tantalum. This is the geometry presently being tested in the 15 000 hour lifetest of reference 12. Also shown in figure 3 are the configurations for the multilayered baffles used in test 2 to separate the erosion rates of the inner and outer, upstream and downstream baffle surfaces and the polished baffles and masks used to obtain erosion profiles. Some of the tests also used removable tantalum pole piece cladding as shown in figure 4 to permit weight measurements and hence calculations of average erosion rates of inner, outer and downstream surfaces.

Facility

It was possible to operate one or two thrusters at the same time by using the mounting frame developed for multiple thruster array (MTA) tests as seen in figure 5.[17] The frame was mounted in the 3.05 m diameter port of the 7.6 m diameter by 21.4 m long vacuum facility at LeRC. To protect thrusters operating at the other end of the tank a 0.46 m by 1.4 m molybdenum shield was installed in the tank at about 14 m downstream of the MTA frame. The bell jar and main tank pressures during multiple thruster operation were in the low to mid 10^{-6} torr range.

Sputtering Rate Measurements

Sputtering rates were measured by documenting the component before and after each test. Different techniques were used to document the various components and these will be described below.

Screen Grid. Sputtering rates of the screen grid were obtained by measuring the grid thickness as a function of radius over three grid diameters (120^{o} apart) using an electronic micrometer. The uncertainty of the measurement was approximately 2.5 μm (0.1 mil). The grid was placed between two probes during the measurement. One probe had a flat surface while the other probe was curved to account for the curvature of the dished grid. In most cases the grids were measured before and after each test. In some instances however screen grid thickness data were available only after the test. But measurement of several unused grids indicated a "thinning out" at the center of the screen grid, due to the dishing process, of about 7.5 μm. This correction was applied to those grids for which there was no initial thickness measurement.

Baffle and pole piece. The baffle sputtering rates were obtained by two methods. The baffles were weighed before and after each test with an analytical balance with an uncertainty of 0.001 g. This method resulted in average sputtering rates per unit area. To obtain radial sputtering profiles of the baffles, iron and tantalum baffles were polished to a mirror finish and then covered by thin half-circle masks made of iron or tantalum as shown in figure 3. After a test a profilometer was used to measure the erosion depth using the masked area as a reference plane. The profilometer measurement had an uncertainty of less than 0.2 μm.

The sputtering rates of the pole piece were obtained by cladding the inside, outside and edge of the pole piece, as shown in figure 4, with thin (1.3 cm wide) tantalum strips. The three pieces were weighed before and after each test. Thus an average sputtering rate per unit area was obtained.

Deposition Rate Measurements

The deposition rates of sputtered material arriving at surfaces inside and outside the thruster from sputtered thruster and facility surfaces were measured by placing small masked quartz slides at various locations. The thickness and composition of the deposited films were obtained by profilometer and spectrographic analyses.

Saturated Ion Current Measurements

For purposes of modeling the sputtering phenomena it was desirable to determine the total incident ion flux rates to critical surfaces. To accomplish this, the screen grid and baffle were electrically isolated from cathode common potential. During thruster operation a variable negative bias was applied to each component and the net ion current to the component measured. The saturated ion current was extrapolated to zero bias to obtain an estimate of the ion current expected during normal operation.

Results and Discussion

For reference a brief description will be given of the internal erosion and deposition-spalling problems observed in the 10 000 hour lifetest.[5] Then, the results of tests conducted at Lewis Research Center to measure and reduce the sputtering rates of the internal thruster components and the associated effects of deposition will be presented. Finally, models which were used to predict the internal erosion rates of the screen grid and baffle and the resulting deposition rates are presented and compared to the experimental results.

Results of the 10 000 Hour Lifetest

During the 10 000 hour lifetest, and during post-test analysis of the thruster, several problems caused by ion sputtering became apparent.[5] Those problems which are discussed in this paper are the erosion of three discharge chamber components and the spalling of that eroded material from the deposition sites.

Screen Grid Erosion

Figure 6 shows the profile of the screen grid, obtained from reference 5, after the 10 000 hour lifetest. The erosion was found to be deepest at the center of the grid where nearly half of the 0.038 cm thick molybdenum grid was sputtered away. Deposited material was found at the outer perimeter. The lifetest thruster (700 series) was operated at a discharge voltage of 37 V and an average beam current of 1.4 A.

An estimate was made of the expected screen grid erosion for the lifetest thruster design over a range of beam currents required by proposed missions (about 0.5 to 2.0 A). From considerations discussed later, the expected screen grid erosion was found to be most severe at the highest (2.0 A) beam current and was calculated to be of such magnitude that the screen grid would have eroded to half thickness in only 7300 hours (~260 Å/hr). This criteria (half-thickness) will be used as a somewhat arbitrary definition of a screen lifetime since no difficulties, attributed to the observed screen grid erosion, were experienced during the 10 000 hour lifetest. Screen grid lifetime could be increased by increasing screen grid thickness. However, increased screen grid thickness has been found[13] to drastically degrade thruster performance.

Baffle Erosion

During the lifetest a hole was observed at the center of the baffle after 5845 hours of operation, at an average beam current of 1.64 A. This hole represents an erosion rate of 1250 Å/hr. Reference 8 showed that the downstream side baffle erosion rate increased slightly faster than linearly with beam current while the upstream side was independent of beam current. From tests discussed later, the ratio of downstream to upstream erosion rates for the lifetest geometry was 2.14. Thus a linear extrapolation of the downstream erosion rate to a 2.0 A beam condition (the expected operating point of an EM thruster) added to the upstream erosion rate predicts a maximum erosion rate of 1430 Å/hr or lifetime (wear through) of less than 5100 hours.

Pole Piece Erosion

Post-test examination of the cathode pole piece showed that the 0.76 mm thick downstream edge of the pole piece had eroded to a sharp knife edge.

Spalling

After about 4500 hours of testing "flakes" were noted on the screen grid of the thruster which was tested in a vertical downward position. These flakes were formed by the spalling of deposited material that was sputtered from the screen grid, baffle and pole piece. The size of the flake varied but some had length up to 0.4 cm. Some of the flakes, which fell to the screen grid, caused ion defocusing and subsequent accelerator grid erosion, large high-voltage trip rates, and eventually shorts between the screen and accelerator grids. Other flakes caused a cathode keeper to cathode common short.

Experimental Results of Sputtering Test at LeRC

Documentation[8] of internal erosion prior to the start of the 10 000 hour lifetest led to predicted lifetimes longer than those experienced during the 10 000 hour lifetest. Therefore, additional studies were made in the areas of internal erosion and flake formation and the results are presented below. In reference 8 a modified "400" series thruster with a "400" series baffle mount was used whereas the thruster used in the lifetest, (701), had several design changes including the baffle mount. For the tests presented herein, thrusters with "700" series and "400" series baffle mounts were used.

Screen Grid

Erosion of the screen grids tested in reference 8 could not be detected at the time of that report. In fact, those screen grids had a net weight gains due to deposition at the outer periphery. Upon learning of the extensive screen grid erosion experienced during the lifetest all grids tested at LeRC that had accumulated long test times at known operating conditions on thrusters employing either baffle mount geometry were measured with a sensitive electronic micrometer.

The results of the thickness measurements of screen grids which have accumulated many tests hours under known conditions and tests where grid thicknesses were measured before and after a run are shown in Table II. In many cases the measured erosion was small and nearly equal to the uncertainty of the measurement. Therefore the erosion rates presented are maximum or "worst case" values. The last column of this table gives the expected minimum lifetime (to erode to half thickness at a 2.0 A beam current) for each test configuration. Test 1 is the 10 000 hour lifetest already discussed and shows the erosion rates for the center of the grid (177 Å/hr actual and 260 Å/hr for a linear extrapolation to a 2.0 A beam current). Test 2 results are for a grid used on a thruster similar to the life test thruster and operated at a beam current of 2 A and a discharge voltage of 37 V. A maximum erosion rate of 280 Å/hr was measured which is in good agreement with the life test result. The grid set used in the tests of reference 8 and shown as test 3 was tested on the same thruster used for test 2 with the exception of the cathode assembly which had the "400" series geometry baffle mount. The erosion rate for the center of the grid was only 110 Å/hr. Of the accumulated 1840 hours, 430 hours of operation were at reduced discharge voltages of 33 and 35 V, resulting in a lower sputtering rate then would be expected at a discharge voltage of 37 V. Therefore, test 4 was conducted at the nominal conditions of test 3 using the grid of test 2 on thruster 802A with a "400" series baffle mount. The resultant screen grid erosion rate was 125 Å/hr, about half that obtained for tests 1 and 2 with the "700" series baffle mount. Thus, these tests indicated that the geometry of the baffle mount played an im-

portant role in determining the screen grid erosion rates. A sputtering model (to be shown later) predicts that approximately 70 percent of the screen grid erosion to be caused by doubly charged ions. Through the use of a beam ion charge analyzer, a higher value of centerline doubly charged ion content was found to exist when a thruster was operated with the 700 series baffle mount.[18] These measurements have also indicated that double ion content of a thruster may vary due to mass utilization efficiency at given operating parameters. Therefore, in comparing results such as found on Table II, the efficiency should be considered in addition to the electrical parameters of the thruster. Since thruster operation at lower discharge voltage results in a lower energy with which an ion strikes a surface, reduced screen grid erosion should occur. In Test 5 a thruster with a 700 series baffle mount was operated at a discharge voltage of 33 V. The sputtering rate was reduced by nearly a factor of three from that measured at 37 V. Likewise, operation of a thruster with a 400 series baffle mount at 35 V reduced the erosion rate for that configuration by about 30 percent.

Figure 7 shows the variation of erosion rate as a function of radius for screen grids operated with each baffle mount geometry. The screen grid operated with the 400 series baffle mount had a maximum erosion rate nearly three times less than the other grid. The total weight loss rate for each screen grid profile was estimated from figure 7 to be 0.82 and 1.2 mg/hr for the 400 and 700 series baffle mounts, respectively.

Thus, screen grid lifetimes of 15 000 hours or more may be achieved by using the 400 series baffle mount at discharge voltages of 37 V or less or the 700 series baffle mount at discharge voltages of 33 V or less.

Baffle

Table III presents the results of tests of baffle erosion for the two types of baffle mounts and for two baffle materials. The average erosion rates were obtained from weight loss measurements whereas the maximum rates were determined by profileometer measurements. For the 700 series mount tests conducted at a beam current of 2.0 A and discharge voltage of 37 V, the total maximum erosion rate was 1320 Å/hr. This rate was nearly equal to the rate (1430 Å/hr) predicted by extrapolation of the 10 000 hour lifetest data to the 2.0 A condition. The use of tantalum cladding which cover the required magnetic iron baffle reduced the maximum erosion rate from 1320 Å/hr to 324 Å/hr. It was observed that with the use of tantalum cladding the upstream and downstream rates were nearly equal. For iron baffles the maximum downstream erosion rate was always about twice the maximum upstream rate at these operating conditions. Weight measurements of upstream iron baffles consistently showed net gains. This was due to deposits on the outer portions of the baffle. This effect was never observed with tantalum baffles.

Figure 8 is an electron scanning photomicrograph of the outer portion of the upstream side of an iron baffle used in test 2. The surface exhibits cone formations which are similar to those found in certain sputter-deposition processes.[19] Analysis of this surface indicated the presence of a deposit of tantalum, molybdenum and tungsten. Apparently, these low sputter yield materials acted as "seed" and provided conditions for cone formation. The buildup of cones apparently inhibited the sputtering of the outer area of the iron upstream baffle. Since tantalum has the lowest sputter yield of the materials used in the thruster there was no "seed" material available hence cone formation was neither expected nor observed on the tantalum surfaces.

Accurate sputter yields for tantalum and iron at low ion energies are difficult to obtain. Use of the values given in the literature indicate that the linear depth erosion rates for tantalum should be greater than for iron at thruster operating conditions of 37 V discharge voltage and beam current of 2 A. However, the depth erosion rates for tantalum were found to be about eight times less than those for iron in the thruster tests. The reason for this is not entirely clear, but mercury adsorption by the tantalum baffle surface may account for the difference. The erosion rates of both iron and tantalum baffles decreased as expected with reductions in the discharge voltage.

Downstream baffles of various materials were tested with a 400 series baffle mount in order to compare their actual erosion rates in a thruster with those expected from the theoretical model and published sputter yields. Table IV lists the measured erosion rates and the calculated erosion rates for discharge voltage of 37 V. With the exception of tantalum, all other materials tested show reasonable agreement between measured and calculated erosion rates.

Other observations were made during these baffle tests. One was that when multiple layered baffles, as shown in figure 3 were used, the thin exposed edge of the iron baffle eroded at relatively high rates (approximately 1200 Å/hr). When this edge was covered with tantalum foil the rate was reduced, as expected, by nearly a factor of seven but was still high when compared to other baffle surfaces. Another observation was that the tantalum upstream center plug, shown in figure 3 used to secure the tantalum baffle assembly to the 700 series baffle mount, eroded at rate about two times faster than that of the downstream surface and about two times faster than the upstream surface when the plug was not used.

The erosion profiles of a tantalum baffle tested at the conditions of the present 15 000 hour lifetest is shown in figure 9. The profiles show peaked sputtering rates at the center of the baffle especially for the upstream side of the baffle. Table III shows that the average erosion rate for the downstream baffle surface of test 11 to be greater than the maximum erosion rate experienced in test 13. This occurs because tests 4, 11 and 12 used the ENT design tantalum baffle in which the downstream and edge surfaces are one piece (see fig. 3). Thus, the weight loss measurements include the edge losses, which as mentioned earlier are comparable to the downstream surface weight losses. The profile shows only the downstream surface.

Thus by using the 400 series baffle mount with tantalum clad baffles and operating at a discharge voltage of 36 V the erosion rate for the central portion of the baffle was reduced from the high

value of 1430 Å/hr found in the 10 000 hour lifetest to about 81 Å/hr (26 Å/hr downstream plus 55 Å/hr upstream plug) for the present thruster configuration. For the ongoing 15 000 hour lifetest the expected baffle lifetime is greater than 100 000 hours.

Pole Piece

Weight loss measurements of the thin tantalum bands, shown in figure 4, used to cover the edge of the iron piece for tests 7, 8, and 9 were made. They indicated erosion rates of about 110, 90, and 30 Å/hr of the downstream edge, inner surface and outer surface of the pole piece, respectively. Measurements using the 400 series baffle mount were somewhat lower but did not exhibit the large differences found at the baffle. These erosion rates indicated that a nominal amount of tantalum cladding will prevent erosion of the iron pole piece and reduce the linear depth erosion rates.

Spalling

Table V shows the sputtering rates of the baffle, the pole piece for tests 15 and 16. The measured deposition rates are presented in Table VI at various thruster locations for the same tests. In order that these results may be compared to those expected in flight applications, an estimate was made of the contribution of the materials originating from outside the thruster and this estimate was subtracted from the deposition measurements. The estimate of deposition due to facility back-sputtered material was obtained by measurement of the concentrations of metals such as copper, chromium and nickel which were not present in the thruster. These concentrations also allowed an estimate of the facility deposited iron flux by the use of the known iron ratio in 304 stainless steel - the facility walls (18 to 20 % Cr, 8 to 12 % Ni, 2 % Mn, 65 to 71 % Fe). If non-preferential sputtering of the stainless steel tank walls takes place, the same ratios of these metals should be present inside the thruster. If preferential sputtering occurs as observed in reference 20 the iron contribution may be twice the amount of the nonpreferential case since the sputtering yield of iron at 1 keV Hg ions at glancing angles is 2.3 times greater than that of Ni.[21,22] Analysis of deposits on quartz slides placed outside the thruster indicated that the tank walls are sputtered nearly nonprefentially and that part of the molybdenum found inside the thruster originates from the molybdenum shields which separates thrusters at opposite ends of the facility. The deposition estimates due to the facility appear in Table VI. With the exception of the pole piece region, 40 to 75 percent of the internal deposits orginate from outside the thruster. It is also apparent that for test 15, operated at a discharge voltage of 37 V, the ratio of thruster to tank material deposition is larger than test 16, 33 V, as expected. The last column of Table VI gives the expected internally generated deposition rates for a thruster operating in space at a beam currents of 1.5 and 2.0 A and discharge voltages of 37 and 33 V for tests 15 and 16 respectively. With erosion rates reduced from those experienced in the 10 000 hour lifetest, the deposition rates should also be lower. In addition, the use of grit-blasted wire mesh, at deposition sites, provides a surface to which the deposited material can readily adhere to. Deposited layers of 30 μm have been found to adhere, without spalling, to wire mesh surfaces.[9]

Thrusters 406C, 802A, and 804 were all equipped with screen mesh at the deposition sites to prevent large flakes from spalling from those sites. Those thrusters have accumulated more than 1700, 3420, and 2700 hours, respectively, with no evidence of flake formation.

Theoretical Models

It is apparent that thruster components may undergo sputtering and deposition at the same time depending on their location and electrical potential.[8] Since the measurements presented in this report represent the net flux lost or gained at each surface it is important to be able to determine the magnitude of each effect in order to have a complete understanding of the sputtering-deposition phenomena in a thruster. First a discussion of the sputtering will be presented and then estimates of the deposition flux arriving from major sputtering sources will be made. These estimates will be made for flux arriving from the thruster as well as from the facility outside the thruster.

Sputtering

Sputtering is an extremely complicated phenomena, and no comprehensive sputtering theory has been developed as yet for all ion energy ranges.[23]

The depth erosion rat of a surface may be calculated from the following equation:

$$\dot{t}_s = 3738 \frac{A}{\rho} \sum_{k=1}^{n} \frac{i_k}{k} S_k \qquad (1)$$

where

$\dot{t}_s$	erosion rate, Å/hr
3738	units conversion constant
A	atomic weight of the target material, AMU
ρ	density of target material, g/km^3
k	charge of impinging ion
i_k	ion current density of each charged state, mA/cm^2
S_k	sputter yield of the incident ion, atoms/ion

Use of this equation to calculate sputter erosion rates of internal thruster components requires knowledge of the local ion density and energy for each ion charged state. Also, the assumption is made that, for low values of plasma potential, the sputter yield of a multiply charged ion at a given energy is equal to the yield of a singly charged ion at an energy equal to the product of the number of charges and the given energy. Sputter yields of reference 24 are used for these calculations and are found in Table VII. Additional assumptions have to be made about conditions inside the thruster. The first is that the pressure inside the thruster is too low for back diffusion of sputtered material to be significant. Next, the sputtered surfaces are assumed clean of adsorbed or condensed material. This second assumption may be questionable and probably depends on the thruster component

location and temperature. Wehner[25] has found that temperatures above 300° C are required to keep mercury from condensing or adhering on a surface and interfering with the sputtering of that surface. Screen grid center temperatures have been measured to be 325° C,[26] however, measured outer edge screen temperatures of 200° C would indicate that sputtering of the screen grid in those areas may be reduced. It is also assumed that the angle of incidence of the ion is not a factor in the thruster since the angle of incidence on sputtering yields does not begin until approximately 200 eV,[27] an energy well above those of the impinging ion flux inside a thruster.

Screen Grid

Equation 1 may be used to calcualte the expected maximum center or total screen grid erosion rates as thruster operating conditions are varied. To do this for the screen grid center with a thruster using a 700 series baffle mount, the parameter values required for eq. (1) were obtained as follows. Beam ion current density profiles such as those shown in figure 10 were obtained for thruster 804[18] for singly and doubly charged ions. (For the ion energies used herein, the sputter erosion due to triply charged ions can be neglected. Accurate measurements are not available, but are estimated to account for about 5 to 7% of the total sputtering.) The values of density obtained from the beam probe are assumed to be proportional to the ion densities at the screen grid. The constant of proportionality is the transmission coefficient of the grid set. The physical open area of the screen grid is 0.67. The total ion current to the screen grid of a thruster operating at a beam current of 2.0 A was measured to be about 0.7 A when either baffle mount geometry was used. This gives an effective ion transmission coefficient of 0.74. Thus, the values of ion current density measured in the center of the beam were divided by 0.74 to calculate the ion current density arriving at the center of the screen grid. (The ion current density can also be calculated from plasma properties inside the discharge chamber as measured by probes. This will be discussed later.)

The energy of the ions at the screen grid was assumed to be commensurate with the local plasma potential. Plasma potentials at the screen grid were measured in a thruster, similar to thruster 804, operating at a discharge voltage of 37 V.[18] The plasma potential at the center of the grid was 33.9 V or about 3 V less than the discharge voltage. Off axis the measured plasma potentials near the screen grid decreased to 33 V at half-radius and 23 V near the anode. Thus, the energy of the ions used to determine sputter yields at the center of the screen grid of a thruster using a 700 series baffle mount was 3 V less than the anode voltage. Probe measurements of the 400 series thruster were not available. For this thruster the centerline ion density was nearly equal to the ion current density at half radius of the thruster with the 700 series baffle mount. Therefore, the plasma potential at the screen grid of the thruster with the 400 series baffle mount was assumed to be 4 V less than the anode voltage.

The calculated and measured erosion rates for the screen grid centerline are plotted in figure 11 as a function of anode voltage for thrusters operated with both baffle mount geometries. In both cases, calculated and measured, the erosion rates of the screen grid center are lower when the 400 series baffle mount is used. The reason for this can easily be seen by comparing figures 10(a) and (b). The current density profiles are markedly peaked for thruster 804 with the 700 series geometry baffle mount when compared to the profiles for thruster 901 with the 400 series geometry baffle mount. The total double to single ion current density ratio, at a given discharge voltage, for the two thruster geometries are nearly equal but the centerline double to single ion current density ratio is about 30 percent lower for thruster 901.

The differences between calculated and measured values for each geometry are probably due to the assumptions required to make the calculation and/or screen grid measurement errors.

Knowledge of the total single and double ion current to the screen grid allows a calculation of the total grid erosion rate to be made. The weight loss rate was calculated for thruster, using both the 400 and 700 series baffle mounts, by using a screen grid measured saturated in currents of 0.64 and 0.74 A, respectively. Also used were the total double-to-total ion current ratios of 0.11 and 0.14 to obtain mass loss rates of 0.78 and 1.13 mg/hr. These rates compare within 10% of those values calculated earlier from the erosion profiles of figure 6.

The total current to the screen grid used in the calculating may be obtained several ways. As already mentioned, it may be obtained by measuring the saturated ion current to an isolated screen grid, and it may be obtained from beam ion density profiles taken near the thruster and corrected for an effective open area of the screen grid. A third method is available to obtain the total screen grid current. This is a calculation that is made by using the Langmuir probe measurements of electron density and temperature. The total current to the screen grid may be calculated by the following equation where the Bohm criteria is used to calculate the ion velocity:

$$i_s = 1.11 \times 10^{-14}\, n_e \sqrt{T_e} \left[\frac{1 + \frac{i_2}{i_1}}{1 + \frac{i_2}{\sqrt{2}\, i_1}} \right] \qquad (2)$$

where

i_s screen grid ion current density, A/cm^2

n_e Maxwellian electron density, cm^{-3}

T_e electron temperature, eV

$\frac{i_2}{i_1}$ double to single ion current density ratio

The Langmuir probe measurements of reference 18 for a thruster using a 700 series baffle mount and operating at a beam currentof 2.0 A and a discharge voltage of 37 V were used to calculate a screen grid ion current of 0.52 A. Values of the double-to-single ion density ratios were also obtained as before from reference 28 for the same thruster. The calcuated screen current of 0.52 A from probe meas-

urements is lower than 0.7 A obtained from the saturated ion current measurement to the screen and obtained from probe ion density profiles taken near the thruster and corrected for the appropriate effective open area of the screen grid. It is felt that the two latter methods are more accurate.

Figure 12 predicts screen grid lifetime as a function of beam current for several values of discharge voltage. Lifetime predictions were made by using eq. (1) and assuming a linear variation of the double-to-single ion ratio with discharge voltage and beam current as shown in reference 28. A lifetime of nearly 16 000 hours is predicted for the screen grid of a thruster using a 400 series baffle mount, operating at a beam current of 2.0 A, and with a discharge voltage of 36 V. These are the conditions of the 15 000 hour lifetest. A linear interpolation of the experimental minimum lifetimes presented in Table II for this geometry predicts about 19 000 hours.

Baffle

Calculations, similar to those made for the screen grid, may be made to obtain erosion rates for the downstream side of the baffle. Using the results of reference 8, where the saturated ion current to the downstream side of the baffle was measured to be 0.14 A and an average centerline double-to-single ion current density ratio value of 0.45, yields an average sputtering rate of 250 Å/hr for the iron baffle on a 400 series geometry mount. (Ion energies were assumed this time to be equal to the discharge voltage since no probe measurements were available for this geometry.) This compares to 260 Å/hr rate obtained from weight loss measurements for the same configuration. The saturated ion current was not measured when the 700 series baffle mount was used. It was calculated, from eq. (2) and the values of plasma properties of reference 19, to be only 0.09 A. Since the measured maximum erosion rate of the downstream side of the baffle using the 700 series geometry baffle mount was about three times as great as that obtained when the 400 series mount was used it must be concluded that the calculated ion current density is not correct. It is also possible that the double to single ion current ratio measured outside the thruster is not valid at the baffle even though reasonable agreement was found using this assumption for the 400 series baffle calculation.

Spalling

To accurately predict the deposition rate on thruster components is very difficult. To illustrate the point, one may follow an imaginary atom sputtered from the downstream side of the baffle; it may impact with the screen grid, where its residence time is very short since it will be sputtered away again by an impinging ion. It may retrace its path back to the baffle and repeat its journey to the screen again before it finally finds its final deposition site on some other component. Our aim is not to try to trace the path of one atom but rather in general to find out if the flux of particles from one source affect the sputtering rate of another component.

A cosine distribution of the sputtered material will be assumed. Distribution patterns may deviate from the cosine distribution if the ion energies are changed[22] but for our purpose the cosine distribution approximation will suffice. Other effects such as the multiple sputtering already mentioned and diffusion and ionization of the sputtered material will be neglected.

The deposition rate from a small surface source to a plane is found to be[29]

$$\dot{t}_D = \frac{\dot{m}\, h^2}{\rho\pi(h^2 + \delta^2)^2} \qquad (3)$$

where

$\dot{t}_D$ thickness deposition rate (cm/hr)

$\dot{m}$ mass loss rate from the sputtered surface (g/hr)

h distance from the sputtering source to the center of the deposition plane (cm)

ρ density of material g/cm^3

δ radial distance from a point on the plane to the center of the plane

This equation may be used to estimate the deposition rate from the baffle to the screen grid or to the anode by properly choosing the radial and axial distances.

The deposition rate from a thin ring source to a plane parallel to it may be determined from reference 29.

$$\dot{t} = \frac{\dot{t}_s\, \dot{m}(h^2 + \delta^2 + R^2)h^2}{\rho\pi(h^2 + R^2 + \delta^2 + 2\,\delta\, R)^{3/2}} \times \frac{1}{(h^2 + \delta^2 + R^2 - 2\,\delta\, R)^{3/2}} \qquad (4)$$

where R is the radius of the ring. This equation reduces to eq. (3) if $\delta = 0$

Equation 4 may be used to calculate the deposition rate from the edge of the pole piece to the screen grid or to the anode by again properly choosing the radial and axial distances. A deposition rate of 1.9 Å/hr of iron was calculated for material from the pole piece to the upstream end of the anode for test 15. The analytically measured deposition rate of iron at the upstream anode location is 3.6 Å/hr of which 3.1 Å/hr was estimated to originate from thruster components. However, since no weight loss measurement was made on the pole piece, the calculated anode deposition rate was expected to be somewhat lower than the measured rate.

The calculated deposition rate at the downstream anode location of the Ta from the pole piece and baffle yields a value of 0.18 Å/hr by using eqs. (2) and (3). The measured rate analytically at the corresponding location was found to be 0.16 Å/hr.

These calculations have shown that the equation can predict with some degree of accuracy the deposition rates originating from the baffle. Therefore we can use the same equations to predict the flux of material to the screen grid where flux measurements are very difficult. If an iron baffle were

used and the thruster operated at normal operating conditions a flux of 24 Å/hr is estimated to be arriving at the center of the screen grid. This rate is about 1/10 of the sputtering rate of the screen grid when the "700 series" baffle mount was used. Also, since the sputtering yields of iron are higher than for tantalum, it is concluded that the arriving flux from the cathode region does not appreciably affect the sputtering rate of the screen grid. Similarly one may show that the atom flux rate arriving at the baffle from the screen grid does not appreciably affect the sputtering rates of the baffle and the pole piece.

Deposition rates arriving at the cathode backplate are more difficult to calculate since the sputtering sources do not approach the simple geometric sources assumed before. A very rough estimate may be made by assuming that the sputtered material on the upstream side deposits uniformly across the entire cathode backplate. This total sputtered material at nominal thruster operating conditions on the upstream side was estimated to be about 1.9×10^{-4} g/hr (upstream side of the baffle, 5.2×10^{-5} g/hr, pole piece $1.7/2 \times 10^{-4}$ g/hr, baffle edge $(4.9/2) \times 10^{-5}$ g/hr). The deposition rate calculated from these values is 25 Å/hr. This rate is about 5 times greater than the deposition rates measured with the quartz slides at the same location.

Conclusions

A study was conducted to eliminate or reduce the effects of internal erosion in 30-cm mercury bombardment ion thrusters. The impact of material, geometric and operational variations was investigated. The erosion rates of the baffle and screen grid experienced in the 10 000 hour lifetest were reduced by factors of about 16 and 2.6, respectively, by the thruster geometry and operating conditions of the current 15 000 hour lifetest. For the thruster used in the latter test, the sputtered surfaces were covered with tantalum, the baffle mount design was changed and the discharge voltage was reduced. To solve the spalling problem (found on the 10 000 hour lifetest) deposition sites have been covered with bead blasted roughened surfaces or screen mesh.

Empirical models were generated to predict sputtering erosion and deposition rates. The calculated rates of these models agreed reasonably well with experimental results. The model allows estimates to be made of internal deposition rates expected in space where the effects of facility back-sputtered material are not present.

The results presented herein have identified solutions to the problems of internal erosion experienced in the 10 000 hour lifetest. These solutions extend the expected lifetime of the present Engineering Model Thruster to nearly 20 000 hours.

References

1. Gilbert, J., and Guttman, C. H., "The Evolution of the SEP Stage/SEPS/Concept," AIAA Paper 73-1122, Oct.-Nov. 1973.

2. Masek, T. D., Richardson, E. H., and Watkins, C. L., "Solar Electric Propulsion Stage Design," AIAA Paper 73-1124, Oct.-Nov. 1973.

3. Duxbury, J. H., "An Integrated Solar Electric Spacecraft for the Enke Slow Flyby Mission," AIAA Paper 73-1126, Oct.-Nov. 1973.

4. Burns, R. E., "Radioactive Waste Disposal via Electric Propulsion," AIAA Paper 75-424, Mar. 1975.

5. Collett, C., "Thruster Endurance Test," Hughes Research Labs., Malibu, Calif., NASA CR-135011, May 1976.

6. Nakanishi, S., and Finke, R. C., "9700-Hour Durability Test of a Five Centimeter Diameter Ion Thruster," Journal of Spacecraft and Rockets, Vol. 11, Aug. 1974, p. 560-566.

7. Power, J. L., "Sputter Erosion and Deposition in the Discharge Chamber of a Small Mercury Ion Thruster," AIAA Paper 73-1109, Oct.-Nov. 1973.

8. Mantenieks, M. A., and Rawlin, V. K., "Studies of Internal Sputtering of a 30-cm Ion Thruster," AIAA Paper 75-400, Mar. 1975.

9. Power, J. L. and Hiznay, D J., "Solutions for Discharge Chamber Sputtering and Anode Deposit Spalling in Small Mercury Ion Thrusters," AIAA Paper 75-399, Mar. 1975.

10. Power, J. L., "Accelerated Life Test of Sputtering and Anode Deposit Spalling in a Small Mercury Ion Thruster," TM X-3269, Sept. 1975, NASA.

11. Nakanishi, S., "15 000 Hour Cyclic Endurance Test of an 8 cm Diameter Electron Bombardment Mercury Ion Thruster," AIAA Paper 76-1022, Key Biscayne, Fla., 1976.

12. Collett, C. R., and Bechtel, R. T., "15 000 Hour Endurance Test of a 900 Series 30-cm Engineering Model Ion Thruster," AIAA Paper 76-1020, Key Biscayne, Fla., 1976.

13. Rawlin, V. K., "Performance of 30-cm Ion Thrusters with Dished Accelerator Grids," AIAA Paper 73-1053, Oct.-Nov. 1973.

14. King, H. J., and Poeschel, R. L., "Low Specific Impulse Ion Engine," NASA CR-72677, Feb. 1970.

15. Poeschel, R. L., King, H. J., and Schnelker, D. E., "An Engineering Model 30-cm Ion Thruster," AIAA Paper 73-1084, Oct.-Nov. 1973.

16. Schnelker, D. E. and Collett, C. R., "30-cm Engineering Model Thruster Design and Qualification Tests," AIAA Paper 75-341, Mar. 1975.

17. Rawlin, V. K., and Mantenieks, M. A., "A Multiple Thruster Array for 30-cm Thrusters," AIAA Paper 75-402, Mar. 1975.

18. Vahrenkamp, R. P., Work Performed Under NASA Contract NAS3-19703.

19. Wehner, G. K., and Hajicek, D. J., "Cone Formation on Metal Targets during Sputtering," Journal of Applied Physics, Vol. 42, Mar. 1, 1971, pp. 1145-1149.

20. Dahlengren, S. D., McClanahan, E. D., Johnston, J. W. and Graybeal, A. G., "Microstructure of Sputter-Deposited 304L Stainless Steel," The Journal of Vacuum Science and Technology, Vol. 7, May-June 1970, pp. 398-402.

21. Wehner, G. K., "Surface Composition Changes Under Ion Bombardment," Proceedings of the 8th Annual Scanning Electron Microscope Symposium, IIT Research Institute, 1975, pp. 133-139.

22. Musket, R. G. and Smith, N. P., Jr., "Competition Between Random and Preferential Ejection on High-Yield Mercury-Ion Sputtering," Journal of Applied Physics, Vol. 39, July 1968, pp. 3579-3586.

23. Kaminsky, M., Atomic and Ionic Impact Phenomena on Metal Surfaces, Academic Press, New York, 1965.

24. Askerov, Sh. G. and Sena, L. A., "Cathode Sputtering of Metals by Slow Mercury Ions," Soviet Physics - Solid State, Vol. 11, Dec. 1969, pp. 1288-1293.

25. Stuart, R. V. and Wehner, G. K., "Sputtering Yields at Very Low Bombarding Ion Energies," Journal of Applied Physics, Vol. 33, July 1962, pp. 2345-2352.

26. Mantenieks, M. A., and Serafini, J. S., Unpublished Data.

27. Wehner, G., "Influence of the Angle of Incidence on Sputtering Yields," Journal of Applied Physics, Vol. 30, Nov. 1959, pp. 1762-1765.

28. Poeschel, R. L., "A 2.5 kW Advanced Technology Ion Thruster," CR-134687, Aug. 1974, NASA.

29. Holland, L., Vacuum Deposition of Thin Films, Chapman and Hall, Ltd., London, 1963.

30. Wehner, G. K., "Sputtering Yields for Normally Incident Hg^{+}-Ion Bombardment at Low Ion Energy," Physical Review, Vol. 108, Oct. 1, 1957, pp. 35-45.

TABLE I(a). - SUMMARY OF THRUSTER DESCRIPTIONS AND OPERATING CONDITIONS

Test	Thruster	Grid set	Cathode ass'y	Baffle mount type	Cathode insert[c]		Beam current (A)	Discharge voltage (V)	Discharge losses	Propellant utilization efficiency (%)	Test time (hours)
					Position	Type					
1 (Ref. 5)	701	648	70_	700 C-IV	R	RF	1.4 average	37	185		10 000
2	406B	36	708[b]	700 C-IV	R	RF	2.0	37	185	----	2 066
3	406A	32	414A	400 C-IV	R	RF	"	37[a]	185	----	1 841
4	802A	36	811A	400 C-IV	F	I	"	37	185	95.0	605
5	802A	39	801	700 C-IV	R	I	"	39	195	91.0	574
6	802A	36	811	400 C-IV	R	I	"	35	185	91-92	976
7	406B	"	708	700 C-IV	R	RF	"	37	185	96.2	165
8	"	"	"	"	R	RF	"		"	~96	238
9	"	"	"	"	R	RF	"	"	"	96.1	324
10	"	"	"	"	R	RF	"	"	"	95-96	95
11	804	804	812A	400 C-IV	F	I	"	36	191	94.4	63
12	804	804	812A	400 C-IV	F	I	"	35	185	93.7	613
13	802A	802	811A	"	F	I	"	36	191	----	419
14	802A	802	811A	400 C-IV	F	I	"	36	191	----	401
15	300A	37		400 CIV	R	RF	1.5	37	185	----	285
16	"	36A		400 CIV	R	RF	2.0	33	185	----	405

[a]Includes 430 hr at discharge voltage of 33 and 35 V.
[b]Includes 149 hr with cathode assembly 414A.
[c]Position: R-recessed, F-flush
Type: RF-rolled foil, I-impregnated.

TABLE I(b). - THRUSTER DESCRIPTION

T/S	Description
406A	"400" series thruster with dished grids, stronger magnetic field and shortened baffle mount. References 13 and 14
701	"700" series EMT. References 5 and 15.
406B	Thruster 406A modified to be equivalent to "700" series EMT
300A	Modified 300 series thruster, like 406A with exception of electromagnets
406C	406B with modifications for internal erosion; like 800 series EMT
802A	"800" series EMT, reference 16 with Ta at erosion sites and screen mesh at deposition sites; like "900" EMT. Reference 12.
804	"800" series modified to be like "900" EMT

TABLE I(c). - BAFFLE AND POLE PIECE GEOMETRY

Test	Baffle configuration	Baffle material				Pole piece Ta cladding
		Downstream	Upstream		Ta edge	
			Outer	Inner		
1	Single	Fe	Fe	Fe	-----	-----
2	Various	Various	-----	-----	-----	-----
3	Various	Various	-----	-----	-----	-----
4,11,12	"900 EMT"	Ta	Ta	Ta	-----	Yes
5	"800 EMT"	Ta	Ta	Ta	-----	Yes
6	Multilayered	Ta	Ta	Ta	Yes	Yes
7	Polished and masks	Ta	Ta/Ta	Ta/Ta	-----	Yes
8	Multilayered	Ta	Ta	Ta	-----	Yes
9	Polished and masks	Ta/Ta	Ta	Ta	-----	Yes
10	Polished and masks	Fe/Ta	Fe/Ta	Fe/Ta	-----	-----
13	Polished and masks	Ta/Ta	Ta	Ta	Yes	-----
14	Polished and masks	Fe/Fe	Ta/Ta	Ta/Ta	-----	Yes
15	Polished and masks	Fe/Ta	Fe/Ta	Fe/Ta	-----	-----
16	Multilayered	Ta	Fe	Ta	-----	-----

TABLE II. - SCREEN GRID SPUTTERING MEASUREMENTS OF VARIOUS THRUSTER CONFIGURATIONS

Test number	Length of test (hr)	Operating conditions				Screen center sputtering rate (Å/hr)	Estimated grid life time (hr)
		ΔVI (V)	J_B (A)	η (%)	eV/ion		
1	10 000	37.0	1.4 avg.	-----		177	11 200
			2.0 extrap.			260 Extrap. to 2 A	7 300
2	2 066	37.0	2.0	-----	185	280	6 800
3	1 840	37.0	2.0	-----	185	110	17 300
4	605	37.0	2.0	94	---	125	15 240
5	574	33,0	2.0	91	185	100	19 000
6	976	35.0	2.0	92	---	80	23 800

E-8957

TABLE III. - BAFFLE SPUTTERING RATES AT BEAM CURRENT OF 2 A

700 SERIES MOUNT

ΔV_I (V)	J_B (A)	Fe Baffle (Å/hr)					Ta Cladding (Å/hr)					
		Downstream		Upstream		Edge	Downstream		Upstream		Plug	Edge
		Average from weight loss	Maximum	Average	Maximum	Average	Average	Maximum	Average	Maximum	Average	
37	1.64 avg.	1250^{1} total										
37	2.0		900^{10}		420^{10}	1200^{8}	137^{9}	154^{9}	111^{7}	170^{7}	320^{8}	
33	2.0						28^{5}		58^{5}			
400 SERIES MOUNT												
37	2.0	256^{3}		64^{3}			44^{4}		23^{4}		88^{4}	
36	2.0	245^{14}	365^{14}				31^{11}	26^{13}	20^{11}	20^{14}	55^{11}	186^{13}
35	2.0						27^{12}		20^{12}		48^{12}	

(Superscript denotes test number.)

TABLE IV. - COMPARISON OF MEASURED AND CALCULATED SPUTTERING RATES OF VARIOUS BAFFLE CLADDING MATERIALS USING THE 400 SERIES BAFFLE MOUNT AT A BEAM CURRENT OF 2.0 A, DISCHARGE VOLTAGE OF 37 V, DOUBLE-TO-SINGLE ION CURRENT RATIO OF 0.45 AND TOTAL DOWNSTREAM ION CURRENT TO BAFFLE OF 0.14 A.

Baffle material	Measured sputtering rate (Å/hr)	Calculated sputtering rate (Å/hr)
Mo	294	210
Fe	256	250
C	311	250
Cu	1180	1750
Ta	30	530

TABLE V. - EROSION RATES OF THRUSTER COMPONENTS FOR TESTS 15 AND 16

Component	Erosion rate (g/hr)	
	Run #15	Run #16
Ta baffle cladding upstream	5.6×10^{-5}	6.2×10^{-5}
Ta baffle cladding downstream	7.0	6.2
Iron baffle edge	45.3	6.4
Ta pole piece outer cladding	---------	2.0
Ta pole piece inner cladding	---------	8.9
Ta pole piece edge cladding	---------	1.2

TABLE VI. - SPECTROGRAPHIC ANALYSIS DATA OF MAJOR CONSTITUANTS OF DEPOSITS AT VARIOUS THRUSTER LOCATIONS

Location	Test No.	Deposition rates (Å/hr)								Dep. rate of estimated tank material	Dep. rate of estimated thruster material
		Cr	Cu	Fe	Hg	Mo	Ni	Ta	Total		
Anode (U.S.)	15	0.26	0.72	4.4	0.2	0.7	0.13	0.25	6.7	2.7	4.0
	16	.17	.48	1.5	.1	.7	.07	.16	3.3	1.7	1.6
Anode (D.S.)	15	----	----	---	---	---	----	----	---	---	---
	16	.25	.59	2.2	.3	1.2	.09	.11	4.7	2.5	2.2
Backplate (Outer)	15	.18	.11	.8	.1	.8	.02	.01	2.0	1.0	1.0
	16	.18	.31	1.46	.1	.6	.03	.01	2.7	1.6	1.1
Manifold	15	.17	.34	1.0	.1	.8	.03	.01	2.5	1.6	.9
	16	.23	.50	1.4	.1	.5	.07	.02	2.9	2.2	.7
Backplate (Inner)	15	.25	.84	8.7	1.1	.6	.09	.17	10.4	2.0	8.4
	16	.05	.22	.7	.1	.4	.07	.52	2.0	.5	1.5
Cathode Backplate	15	.02	.01	4.7	.1	.1	.01	.07	4.9	---	4.9
	16	.01	.05	1.3	.1	.03	.07	2.7	4.3	---	4.3

TABLE VII. - SPUTTER YIELDS OF VARIOUS MATERIALS USED IN THRUSTER SPUTTERING STUDIES (REF. 24)

Material	Ion energy, (V)	Sputter yield (atoms/ion)
Mo	33	2.1×10^{-4}
	66	27.5
Fe	33	3.5
	66	44
C	33	
	66	44[a]
Cu	33	26
	66	330
Ta	33	2.1
	66	63

[a]Ref. 30.

E-8957

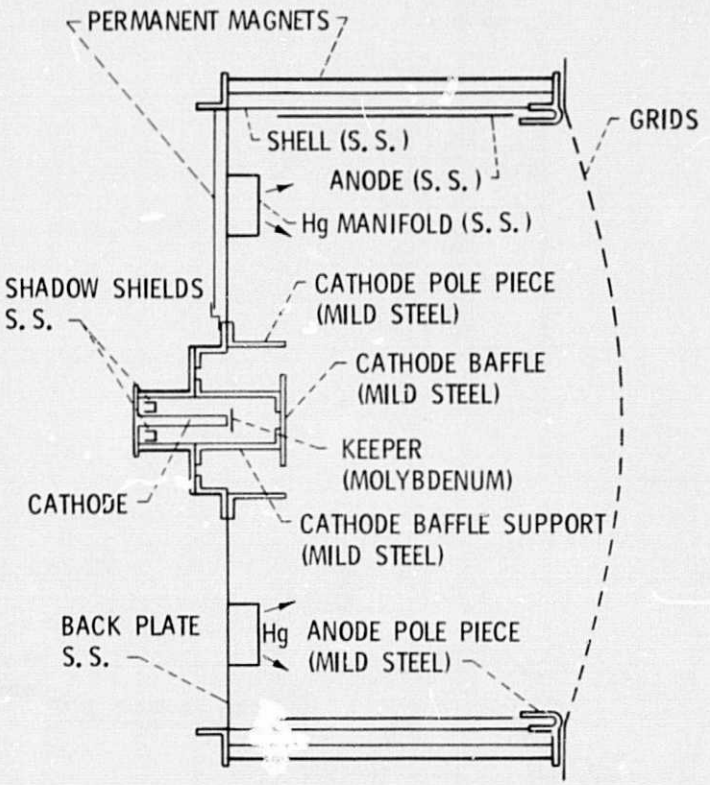

Figure 1. - Cross sectional view of a modified "400 series" 30 cm diameter thruster.

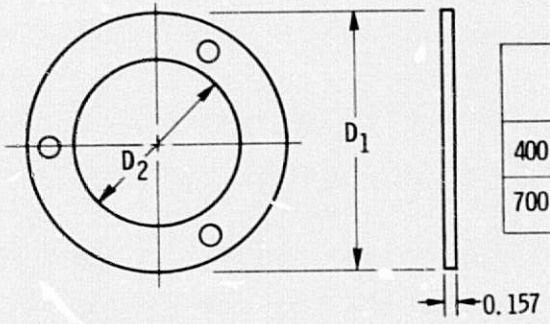

	D_1, cm	D_2, cm
400 SERIES	3.175	2.22
700 SERIES	2.03	1.143

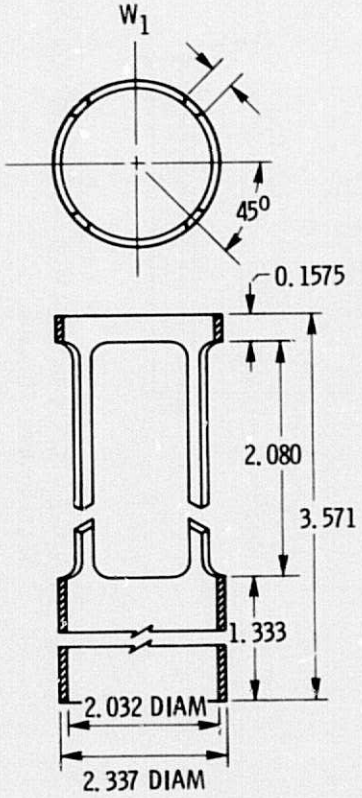

	W_1, cm
400 SERIES	0.635
700 SERIES	0.318

Figure 2. - Baffle support of the 400 and 700 series.

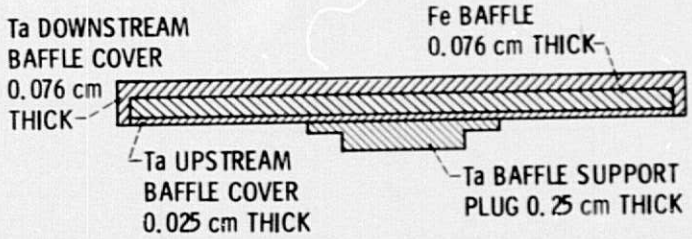

(a) Ta CLAD BAFFLE.

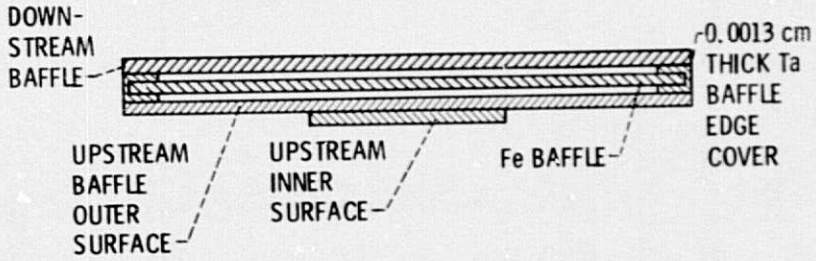

(b) MULTILAYER BAFFLE.

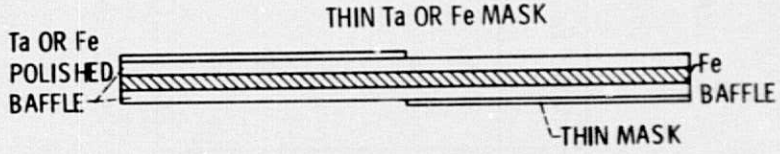

(c) POLISHED BAFFLE.

Figure 3. - Cross section views of baffle geometries tested.

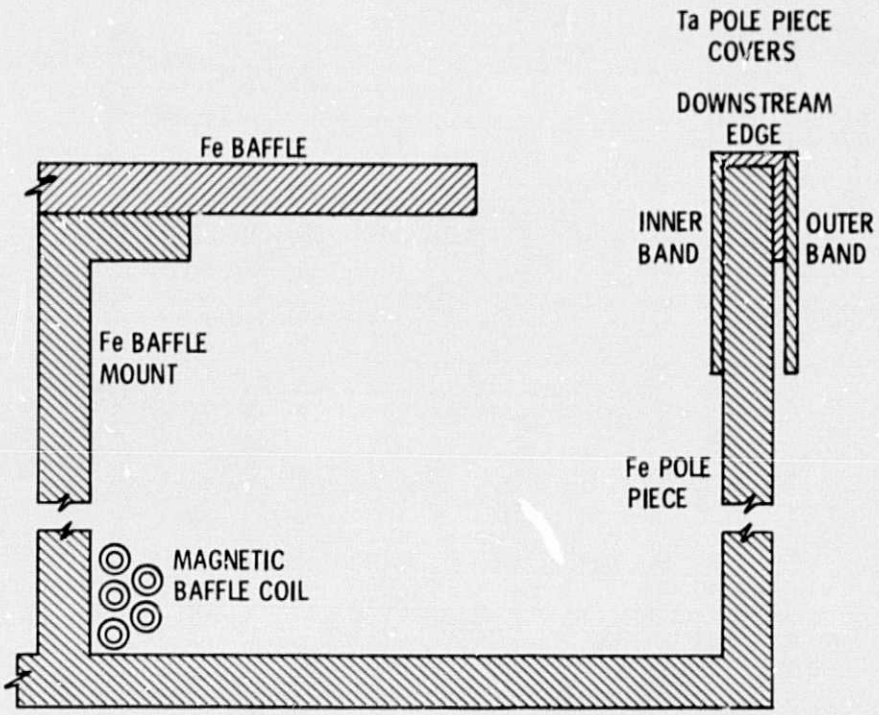

Figure 4. - Cross section view of pole piece cladding.

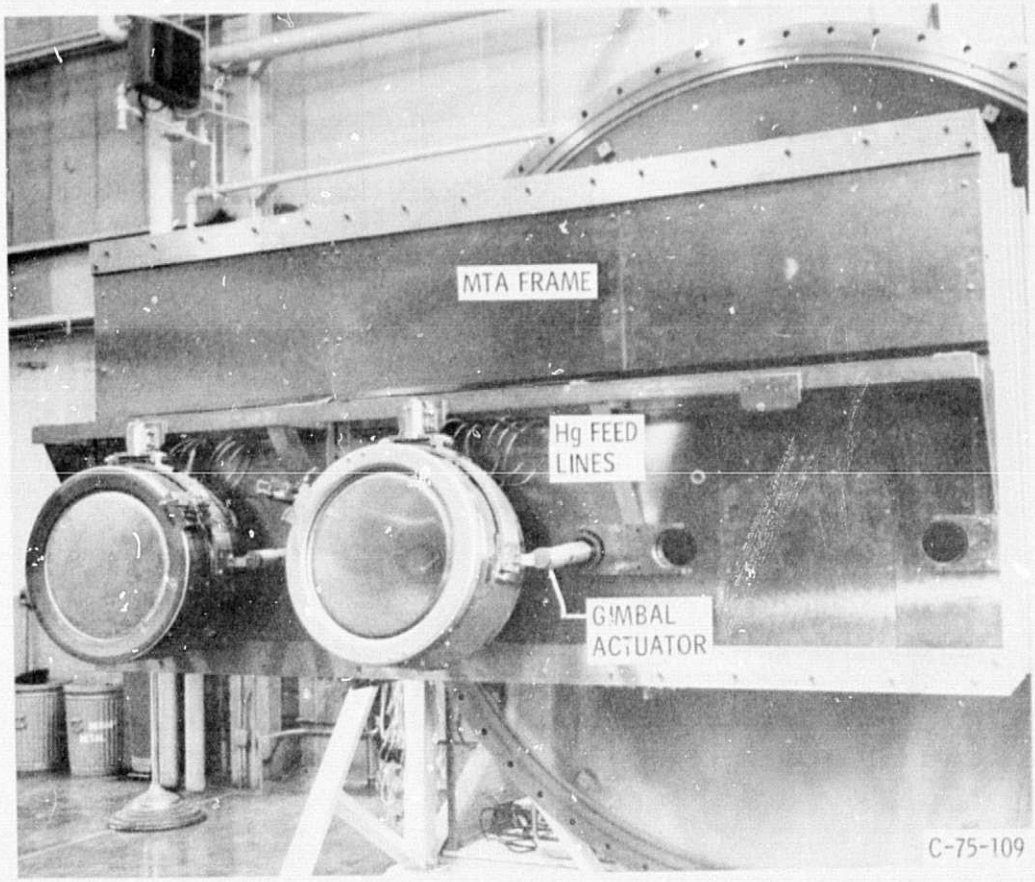

Figure 5. - Two 30-cm Hg ion thrusters mounted on multiple thruster array frame.

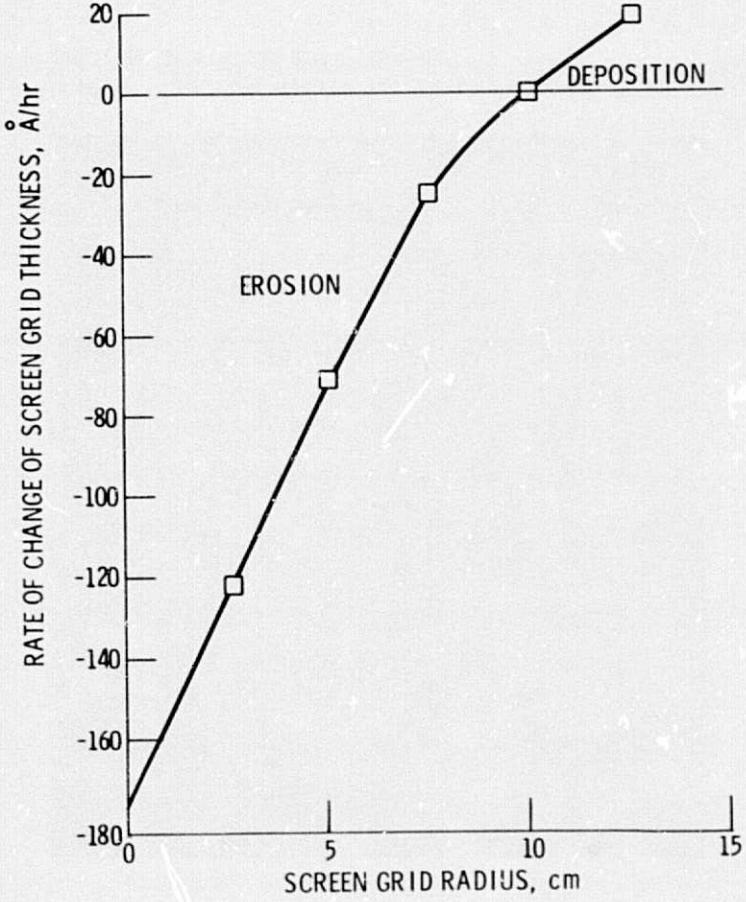

Figure 6. - Screen grid sputtering rate (average) during 10 000 hour life test (ref. 5).

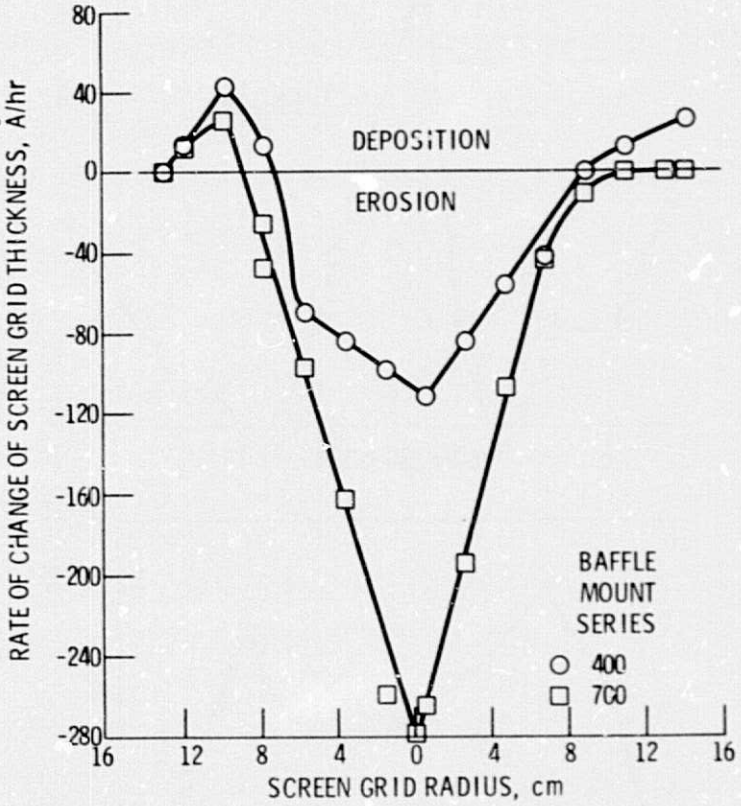

Figure 7. - Screen grid sputtering profiles with 400 and 700 series baffle mounts.

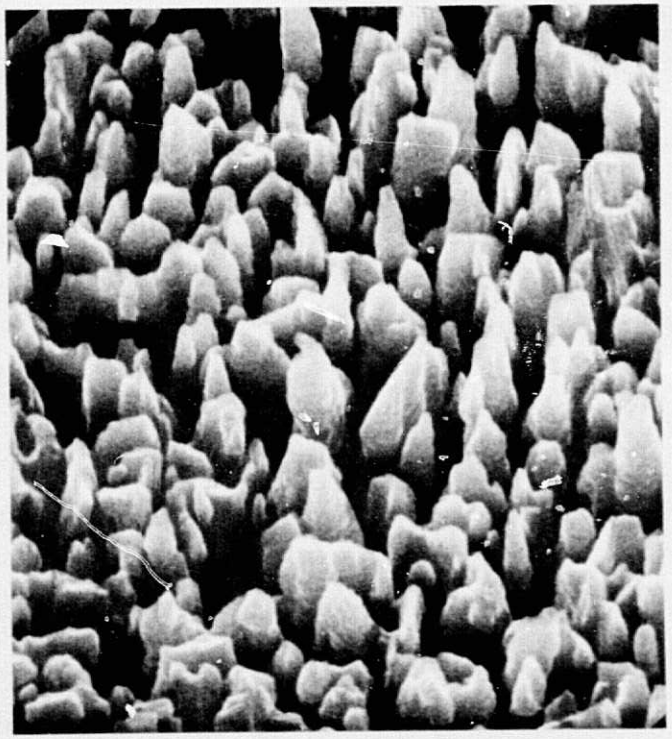

Figure 8. - Scanning electron microscope photograph of cones on upstream side of iron baffle; X10 000.

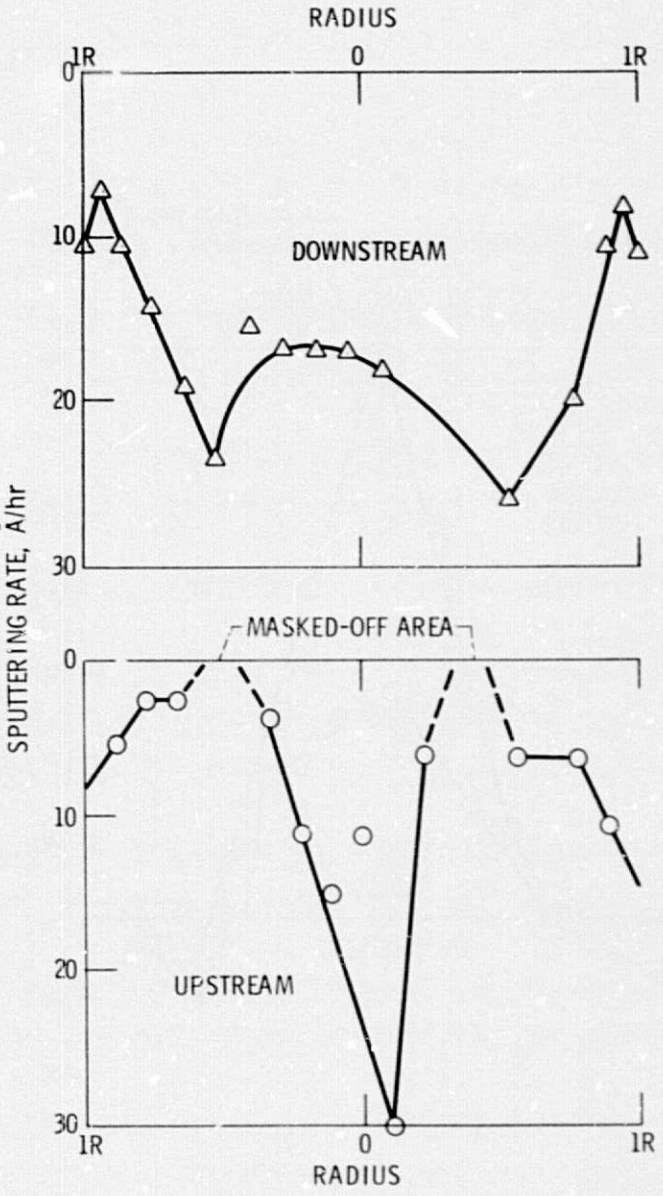

Figure 9. - Sputtering rates of TA clad baffle using the "400 series" baffle mount at $\Delta V_T = 36$ V, $J_B = 2.0$ amperes.

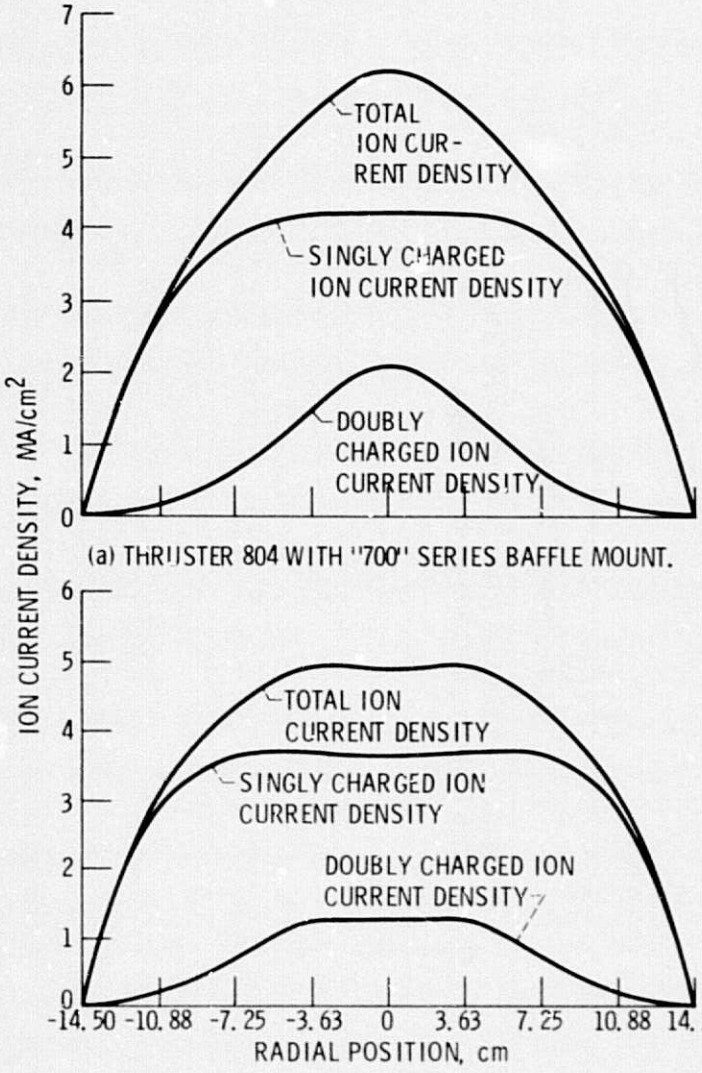

(a) THRUSTER 804 WITH "700" SERIES BAFFLE MOUNT.

(b) THRUSTER 901 WITH "400" SERIES BAFFLE MOUNT.

Figure 10. - Ion beam current densities as a function of radial position. (Beam current 2.0 amp, discharge voltage 35 V, discharge losses 185 eV/ion.)

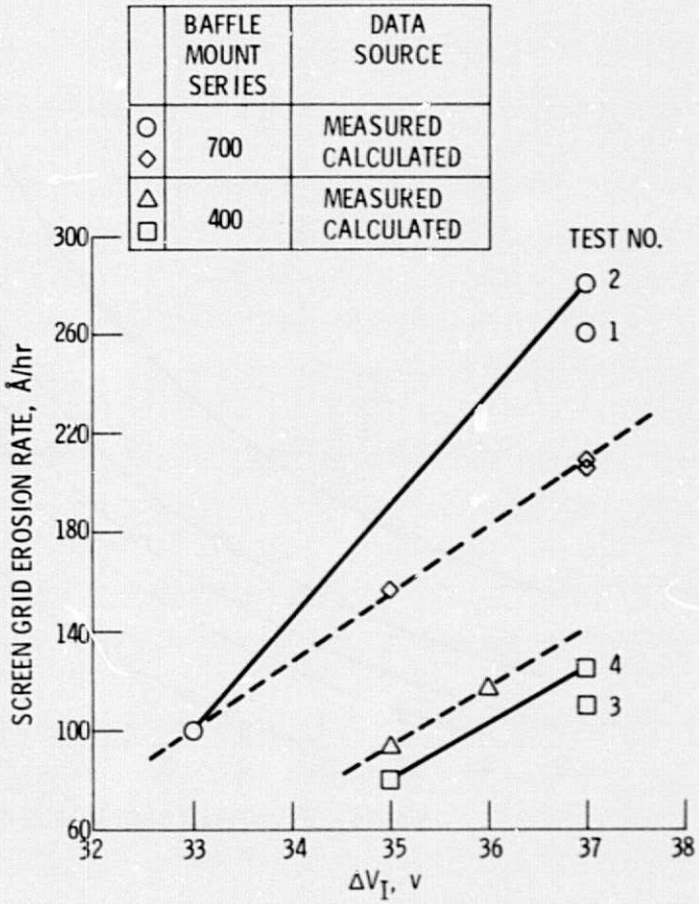

Figure 11. - Screen grid center erosion rates as a function of discharge voltage.

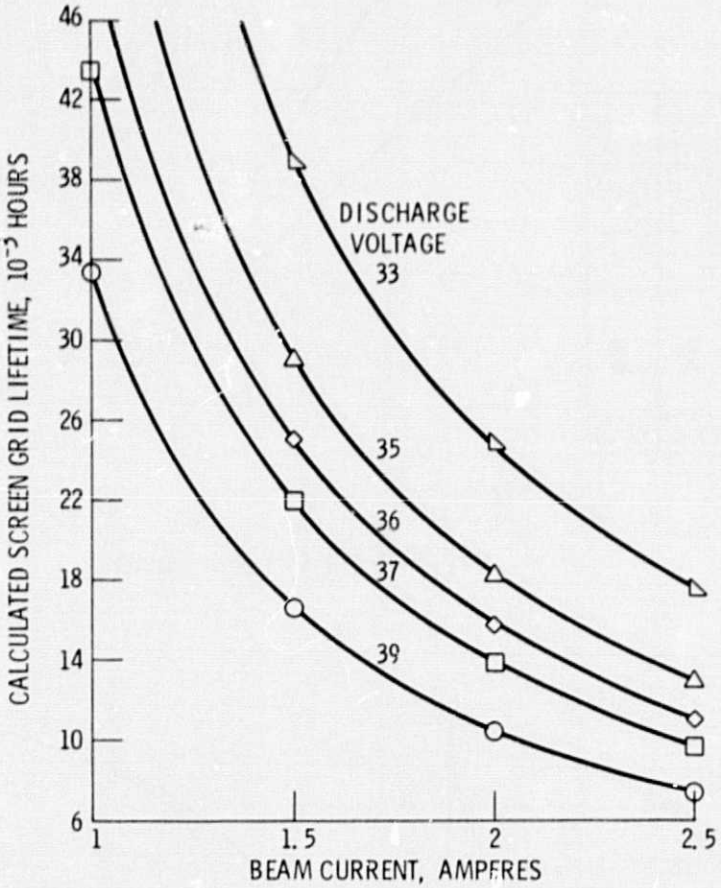

Figure 12. - Calculated screen grid life times as a function of beam current and discharge voltage.

NASA-Lewis